

# Measurement of Pore Size and Matrix Characteristics in Low-k Dielectrics by Neutron Contrast Variation

Ronald C. Hedden, Hae-Jeong Lee, Barry J. Bauer,  
Christopher L. Soles, Wen-li Wu, and Eric K. Lin

*National Institute of Standards and Technology, Polymers Division, Gaithersburg, Maryland 20899*

**Abstract.** The principle of small-angle neutron scattering (SANS) contrast variation is applied to characterization of nanoporous low-k thin films. Using a vapor adsorption technique, SANS measurements are used to identify a "contrast match" solvent mixture consisting of the hydrogen- and deuterium-containing analogs of a probe solvent. The contrast match solvent is subsequently used to conduct SANS porosimetry experiments. In combination with information from X-ray reflectivity and ion scattering, the technique is useful for estimating the density of the matrix (wall) material and the pore size distribution. To illustrate the technique, a porous methylsilsequioxane (MSQ) spin-on dielectric is characterized.

## INTRODUCTION

Much of the recent developmental efforts in low-k dielectrics involve production of nanoporous thin films. By using synthetic techniques that leave nanometer-sized ( $< 10$  nm) pores in the film, the resultant dielectric constant can be reduced to unprecedented levels. The nanoporosity not only lowers the average dielectric constant, but also changes the strength, permeability, and other crucial properties of the films. Therefore, it is necessary to characterize the nature of the porosity to guide the synthetic efforts and to correlate a variety of electrical and mechanical properties.

The National Institute of Standards and Technology (NIST) Polymers Division previously developed a method of measuring pore volume fraction, matrix density, average pore size, and coefficient of thermal expansion by using a combination of techniques: small angle neutron scattering (SANS), specular x-ray reflectivity (SXR), and ion scattering [1-2]. In addition, SANS contrast variation or contrast matching is a powerful scattering technique that we have recently applied to low-k films. In conjunction with SXR and ion scattering measurements, contrast variation permits assessment of matrix mass density, matrix homogeneity, and pore size distribution [3]. This report illustrates the experimental methods, data analysis, and limitations of the SANS contrast variation technique.

## MATERIALS AND MEASUREMENT TECHNIQUES\*

The nanoporous dielectric was an organosilicate spin-on type (polymethylsilsequioxane, MSQ) on a silicon substrate obtained from International Sematech. Atomic composition was obtained by ion scattering [1-2].

### Small Angle Neutron Scattering

SANS measurements were conducted at the NIST Center for Cold Neutron Research 8m facility (Gaithersburg, MD) [4]. The neutron wavelength was  $\lambda = 6$  Å with a spread of  $\Delta\lambda/\lambda = 0.12$ , and sample to detector distance was 384 cm, giving a useful range of scattering vector ( $0.012 < q < 0.14$ ) Å<sup>-1</sup>. Data were analyzed by established methods with the software provided by the Center for Neutron Research at NIST [5]. Films were enclosed in a vacuum-tight flow

---

\* Certain commercial materials and equipment are identified in this paper in order to adequately specify the experimental procedure. In no case does such identification imply recommendation by the National Institute of Standards and Technology nor does it imply that the material or equipment is the best available for this purpose.

cell with quartz windows. Scattering from 10 identical films was simultaneously measured to increase the coherent scattering intensity. A mixture of toluene- $h_8$  and toluene- $d_8$  (saturated vapors in air) was delivered to the flow cell using two syringe pumps equipped with 100 cm<sup>3</sup> syringes. Each syringe contained a small amount of liquid toluene in equilibrium with its saturated vapor. For porosimetry experiments, one syringe was filled with air and the other was filled with an  $h_8/d_8$  toluene mixture of the contrast match composition.

## Specular X-ray Reflectivity

Specular X-ray reflectivity (SXR) was measured using a high-resolution reflectometer capable of characterizing films up to 1.5  $\mu$ m thick [1]. In the specular condition, data are collected with the grazing incident angle equal to the detector angle, and the reflected intensity is recorded as a function of incident angle. The film thickness, surface roughness, and electron density profile are deduced using computer modeling to fit the experimental SXR data. To measure solvent (toluene) uptake as a function of partial pressure, SXR experiments were conducted inside an environmental control chamber equipped with X-ray transparent Be windows. A custom-built vapor delivery apparatus consisting of two mass flow controllers delivered mixtures of dry air and saturated toluene vapor to the chamber at a total flowrate of 500 cm<sup>3</sup> min<sup>-1</sup> [6]. The measured electron density profile was used to deduce the volume fraction toluene uptake at each partial pressure.

Uncertainties in all SANS and SXR data are calculated as the estimated standard deviation of the mean, based on the goodness of a least squares fit to the data. Similar uncertainties exist in quantities calculated from fitted parameters. The total combined uncertainty is not given, as comparisons are made with data obtained under the same conditions. In cases where the limits are smaller than the plotted symbols, the limits are left out for clarity.

## RESULTS AND DISCUSSION

### Contrast Match Point Determination

Contrast matching involves identification of a solvent having the same neutron scattering length density as the matrix of the porous material. Until

now, SANS contrast matching has not been widely applied to the study of nanoporous dielectric thin films because of experimental complications. Because the low- $k$  films are usually about 1  $\mu$ m or less in thickness, immersing the films in liquid solvent results in substantial incoherent background scattering from the solvent that overwhelms the coherent scattering from the films (containing the structural information). However, if the nanoporous films are instead exposed to saturated solvent vapor, all accessible pores are filled with liquid solvent by capillary condensation without filling the sample cell with excess solvent.

Pores are therefore filled with a mixture of hydrogen and deuterium containing solvents by exposure to saturated solvent vapor. All accessible pores are filled by liquid, and their neutron contrast changes. The composition of the solvent mixture is varied until a minimum in the scattered intensity is observed. For a material with a matrix of homogeneous atomic composition, the scattered neutron intensity is proportional to the difference in the scattering length densities between the wall and the pores squared:

$$I(q) \propto (\rho_m - \rho_s)^2 \quad (1)$$

In Eqn. 1,  $\rho_m$  and  $\rho_s$  are the mass densities of the matrix (wall) and the solvent,  $q$  is the scattering vector, and neutron contrast factor  $\Delta$  is defined by:

$$\Delta = \frac{\sum_i n_i b_i}{\sum_i n_i m_i} \quad (2)$$

Sums are taken over a unit mass in the sample;  $n_i$  is the number of a given nucleus,  $b_i$  is the scattering length of the nucleus, and  $m_i$  is its mass. The solvent composition at which  $I(q)$  is minimized is the "match point" where the contrast factor of the wall is the same as that of the solvent. For a material with homogeneous matrix, the coherent scattered intensity tends to zero over all  $q$  when the pores are filled with solvent of the contrast match composition. For a material with inhomogeneous atomic composition in the matrix, the dependence of  $I(q)$  on solvent composition is more complicated.  $I(q)$  will be non-zero at all compositions, and multiple minima in  $I(q)$  may be observed as composition is varied.

The contrast match point determination was done for the MSQ dielectric here using toluene as a probe solvent. Because toluene does not have any substantially acidic protons under the conditions employed, the risk of proton or deuteron exchange between solvent and sample is minimized. The toluene is also able to wet the surface of most

organosilicate dielectrics, facilitating condensation of liquid in the pores.

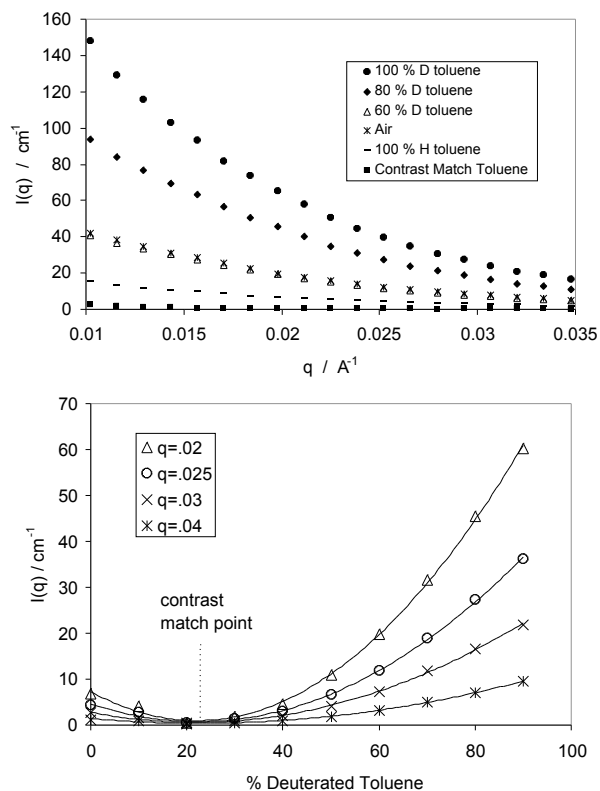


**FIGURE 1.** Determination of the contrast match point of an MSQ type spin-on low-k dielectric.

Figure 1 illustrates the determination of the contrast match point. The composition of the saturated solvent vapor was varied incrementally from 100 % toluene- $d_8$  to 100 % toluene- $h_8$ , changing the scattering length density of the liquid in the pores. As the solvent composition was varied, the scattered intensity changed, but the overall shape of the data remained the same. Exposure of the sample to solvent therefore did not deform the sample or change its morphology. The scattered intensity passes through a minimum at a composition near (22.5 %  $d_8$ , 77.5 %  $h_8$ ) toluene. Near the match point, very little scattering remains, indicating that the matrix is essentially of homogeneous atomic composition on a nanometer length scale. If there were non-uniformities in the matrix, residual coherent scattering would be observed for all solvent compositions. The existence of a true match point also verifies that all pores are open (accessible) to toluene.

From the contrast match point determination, matrix mass density can be assessed by setting  $I(q) = 0$  and rearranging Eqn. 1. The scattering length density (SLD) of the solvent, ( $\rho_s \rho_s$ ), is known, and it equals

the SLD of the matrix ( $\rho_m \rho_m$ ) at the match point. For the MSQ material in the current study, a value of  $\rho_m = (1.97 \pm 0.11) \text{ g cm}^{-3}$  was found, which is substantially higher than the value of  $(1.58 \pm 0.09) \text{ g cm}^{-3}$  determined by X-ray reflectivity with solvent sorption. (See experimental section for explanation of uncertainties). A possible reason for the discrepancy is that the value of the matrix mass density calculated from the contrast match experiment does not account for the possibility that some of the solvent permeates the matrix. It is possible that the matrix itself can accommodate some amount of solvent, e.g., in small voids or "micropores" with dimensions comparable to the size of a single solvent molecule ( $< 2 \text{ nm}$ ). For example, MSQ type materials contain cagelike organosilicate structures with dimensions comparable to the size of a toluene molecule. If a certain amount of solvent permeates the matrix, filling the micropores, the *total* solvent uptake determined by SXR will include this amount in addition to the solvent that fills the larger mesopores by capillary condensation. (Mesopores are defined as those with dimensions of (2 to 50) nm). In addition, the value of mass density determined from the contrast match experiment, which excludes the contribution will be higher than the bulk density of the matrix material including the voids. Because the SANS and SXR values of matrix density are not affected in the same way by this phenomenon, different values for density may result.

Swelling of the matrix is unlikely to affect the density measurements appreciably, as the sample thickness changed by less than 1 % between dry air and saturated toluene atmospheres.

## SANS/SXR Capillary Porosimetry

In a capillary porosimetry experiment, the nanoporous material is exposed to solvent vapor, and the mass uptake of the solvent is measured as a function of solvent partial pressure. Figure 2 shows toluene uptake (volume fraction  $\rho_v$ ) vs.  $(P/P^*)$  for the MSQ dielectric as measured by SXR [See Ref. 6 for details]. Here,  $P$  is solvent partial pressure, and  $P^*$  is the saturated vapor pressure. The sample has an overall porosity of  $\rho_v = (0.30 \pm 0.01)$ .

Capillary porosimetry is frequently employed in determination of pore size distributions. A major challenge in capillary porosimetry is the conversion of the (mass uptake vs.  $P$ ) data to pore size distribution. Typically, at a given partial pressure  $P$ , pores with dimensions smaller than a critical size  $r$  are assumed to fill with solvent. The dependence of  $r$  on  $(P/P^*)$  is

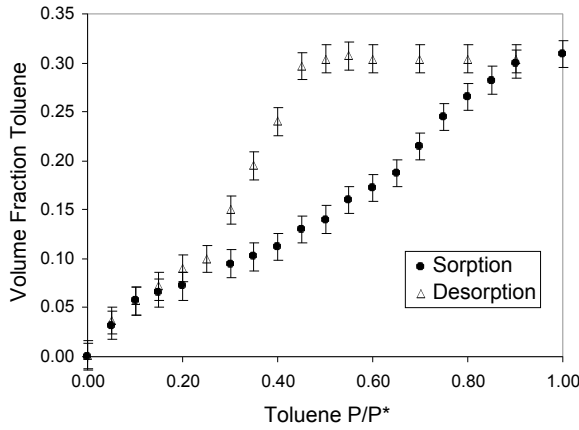


**FIGURE 2.** Volume fraction toluene vs. toluene partial pressure for the MSQ dielectric by specular X-ray reflectivity measurement. See text for explanation of uncertainties.

generally not measured, but  $r$  is calculated from a model instead. A simplified model of pore geometry (such as infinite cylinders) is assumed, and a thermodynamic relation, often the classic Kelvin equation, is used to calculate  $r$  from  $(P/P^*)$ . However, interpretations of pore geometry are usually oversimplified, and the applicability of the Kelvin equation on nanometer length scales is questionable. Capillary porosimetry generally fails to describe the true pore size distribution, providing only qualitative comparisons between samples. In addition, sorption hysteresis phenomena exhibited by most mesoporous materials, as in Figure 2, introduce serious ambiguities in data interpretation.

Capillary porosimetry can be greatly enhanced by introduction of SANS experiments. By using SANS to measure pore size instead of calculating a size  $r$  from a model, pore size can be determined without using the Kelvin equation, and the effects of sorption hysteresis become less important. Once a contrast match solvent mixture is identified, SANS capillary porosimetry experiments can be conducted so that solvent-filled pores have the same SLD as the matrix. The coherent scattering thus contains structural information concerning the unfilled pores. As  $P/P^*$  is varied stepwise, progressively filling pores from smallest to largest, the SANS measurement yields the average size of the unfilled pores. Combining this information with the  $(\xi_c$  vs.  $P/P^*$ ) data from SXR reveals characteristics of the size distribution. Although assumptions must still be made regarding pore geometry to fit the scattering data, these assumptions are less restrictive than those necessary for application of the Kelvin equation.

Figure 3 shows SANS capillary porosimetry data for the MSQ sample using toluene of the match point

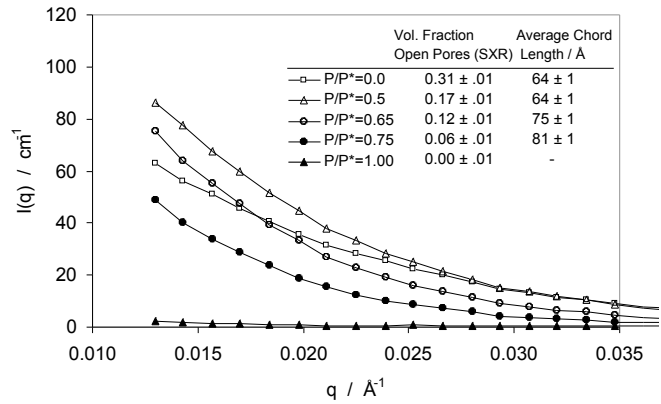


**FIGURE 3.** SANS Contrast Match Porosimetry experiments on a nanoporous random two-phase material. As partial pressure  $P/P^*$  is varied, the average size is measured for different sub-populations of pores. Lines are fits to Eqn. 3. See text for explanation of uncertainties.

composition. Starting from  $(P/P^* = 0)$ , pure air, the sample was exposed to increasing toluene partial pressure  $P$  in a fashion analogous to the sorption experiment in Figure 2. As the solvent partial pressure  $P$  was increased incrementally to  $P^*$ , the pores filled via capillary condensation, and the coherent scattering was gradually eliminated. Generally speaking, pores fill from smallest to largest as  $P/P^*$  is increased, although the filling order can be a complicated function of the local geometry in the material. Each value of  $P/P^*$  yields a measurement of the average size of the unfilled pore population. Assuming the smallest pores fill at a given partial pressure, leaving the larger pores open, one can in principle extract the pore size distribution in this fashion.

To obtain an average unfilled pore size for the current material, scattering data were analyzed by the Debye equation[8]:

$$I(q) = \frac{8 \Delta \rho_p (1 - \Delta \rho_p) (\Delta \rho_m \Delta \rho_s)^2 \bar{V}^3}{(1 + \bar{V}^2 q^2)^2} \quad (3)$$

The Debye equation describes scattering from random two-phase materials, and is an appropriate model for the present sample judging by the goodness of the fits. For each partial pressure  $P$ , a correlation length  $\bar{V}$ , a domain size for the material averaged over both phases, was computed by non-linear least squares regression. The average chord length through the pores is then given by  $l_c = (\bar{V}/(1 - \Delta \rho_p))$ , where  $\Delta \rho_p$  is the volume fraction of unfilled pores, obtained here from SXR measurements. The inset to Figure 3 illustrates how average chord length varies with unfilled volume fraction. When all of the pores are unfilled, the average chord length is  $(64 \pm 1) \text{ \AA}$ . As pores are filled, the average chord length increases, reaching  $(81 \pm 1) \text{ \AA}$  when  $\Delta \rho_p = 0.06$  (20 % of the pores remain

unfilled). (Uncertainties only consider the goodness of the least squares fits to the data, and the total combined uncertainty from all sources is likely to exceed quoted values).

For the randomly structured MSQ material studied here, the ( $l_c$  vs.  $\Delta_p$ ) data presents some sense of the width and upper limit of the pore size distribution. However, deconvolution of the size information to give an explicit pore size distribution is a challenging problem that cannot be addressed presently. Describing the capillary condensation process as a function of  $P/P^*$  for a randomly structured material is inherently difficult due to the lack of a well-defined pore dimension and unknown pore geometry. Construction of an explicit size distribution may be more straightforward for samples with pores of spherical or other simple geometry.

## ACKNOWLEDGMENTS

We thank International Sematech for providing the sample and for financial support, and the Office for Microelectronics Programs at the National Institute of Standards and Technology for financial support. We acknowledge the support of the National Institute of Standards and Technology, U.S. Department of Commerce, in providing the neutron research facilities used in this work. Dr. Hedden acknowledges the support of a National Research Council postdoctoral fellowship.

## REFERENCES

1. Wu, W.-L., Wallace, W.E., Lin, E.K., Lynn, G.W., Glinka, C.J., Ryan, E.T., and Ho, H.M., *J. Appl. Phys.* **87:3**, 1193-1200 (2000).
2. Bauer, B.J., Lin, E.K., Lee, H.J., Wang, H., and Wu, W.-L., *J. Electron. Mater.* **30:4**, 304-308 (2001).
3. Hedden, R.C., Bauer, B.J., Lee, H.-J., and Wu, W.-L., *Abstr. Pap. Am. Chem. Soc. (PMSE)* **224**, 120-PMSE Parts 2 (2002).
4. Prask, H.J., Rowe, J.M., Rush, J.J., and Schröder, I.G.J., *Res. Natl. Inst. Stand. Technol.* **98**, 1 (1993).
5. Hammouda, B., Krueger, S., and Glinka, C.J., *Res. Natl. Inst. Stand. Technol.* **98**, 31 (1993).
6. Lee, H.J., Soles, C.L., Liu, D.W., Bauer, B.J., and Wu, W.-L., *J. Polym. Sci. Part B-Polym. Phys.* **40(19)**, 2170-2177 (2002).
7. *Polymers and Neutron Scattering*, Higgins, J. S. and Benoit, H. C., Oxford: Claredon Press, 1994.
8. Debye, P., Anderson, H.R., and Brumberger, H. J., *Appl. Phys.* **28**, 679 (1957).